



HAL
open science

The Werner syndrome protein affects the expression of genes involved in adipogenesis and inflammation in addition to cell cycle and DNA damage responses.

Ramachander V. N. Turaga, Eric R. Paquet, Mari Sild, Julien Vignard, Chantal Garand, F. Brad Johnson, Jean-Yves Masson, Michel Lebel

► To cite this version:

Ramachander V. N. Turaga, Eric R. Paquet, Mari Sild, Julien Vignard, Chantal Garand, et al.. The Werner syndrome protein affects the expression of genes involved in adipogenesis and inflammation in addition to cell cycle and DNA damage responses.. *Cell Cycle*, 2009, 8 (13), pp.2080-2092. 10.4161/cc.8.13.8925 . hal-02655604

HAL Id: hal-02655604

<https://hal.inrae.fr/hal-02655604v1>

Submitted on 29 May 2020

HAL is a multi-disciplinary open access archive for the deposit and dissemination of scientific research documents, whether they are published or not. The documents may come from teaching and research institutions in France or abroad, or from public or private research centers.

L'archive ouverte pluridisciplinaire **HAL**, est destinée au dépôt et à la diffusion de documents scientifiques de niveau recherche, publiés ou non, émanant des établissements d'enseignement et de recherche français ou étrangers, des laboratoires publics ou privés.




The Werner syndrome protein affects the expression of genes involved in adipogenesis and inflammation in addition to cell cycle and DNA damage responses


Ramachander V.N. Turaga, Eric R. Paquet, Mari Sild, Julien Vignard, Chantal Garand, F. Brad Johnson, Jean-Yves Masson & Michel Lebel


To cite this article: Ramachander V.N. Turaga, Eric R. Paquet, Mari Sild, Julien Vignard, Chantal Garand, F. Brad Johnson, Jean-Yves Masson & Michel Lebel (2009) The Werner syndrome protein affects the expression of genes involved in adipogenesis and inflammation in addition to cell cycle and DNA damage responses, *Cell Cycle*, 8:13, 2080-2092, DOI: [10.4161/cc.8.13.8925](https://doi.org/10.4161/cc.8.13.8925)


To link to this article: <http://dx.doi.org/10.4161/cc.8.13.8925>

 Published online: 01 Jul 2009.

 Submit your article to this journal [↗](#)

 Article views: 283

 View related articles [↗](#)

 Citing articles: 21 View citing articles [↗](#)

Report

The Werner syndrome protein affects the expression of genes involved in adipogenesis and inflammation in addition to cell cycle and DNA damage responses

Ramachander V.N. Turaga,¹ Eric R. Paquet,¹ Mari Sild,¹ Julien Vignard,¹ Chantal Garand,¹ F. Brad Johnson,² Jean-Yves Masson¹ and Michel Lebel^{1,*}

¹Centre de Recherche en Cancérologie de l'Université Laval; Hôpital Hôtel-Dieu de Québec; Québec City, QC CA; ²Department of Pathology and Laboratory Medicine; University of Pennsylvania; Philadelphia, PA USA

Key words: Werner syndrome, aging, microarray, adipogenesis, inflammation, cell cycle, DNA repair

Werner syndrome (WS) is characterized by the premature onset of several age-associated pathologies. The protein deficient in WS (*WRN*) is a RecQ-type DNA helicase involved in DNA repair, replication, telomere maintenance and transcription. However, precisely how *WRN* deficiency leads to the numerous WS pathologies is still unknown. Here we use short-term siRNA-based inhibition of *WRN* to test the direct consequences of its loss on gene expression. Importantly, this short-term knock down of *WRN* protein level was sufficient to trigger an expression profile resembling fibroblasts established from old donor patients. In addition, this treatment altered sets of genes involved in 14 distinct biological pathways. Besides the already known impact of *WRN* on DNA replication, DNA repair, the p21/p53 pathway, and cell cycle, gene set enrichment analyses of our microarray data also uncover significant impact on the *MYC*, *E2F*, cellular *E2A* and *ETV5* transcription factor pathways as well as adipocyte differentiation, *HIF1*, *NFκB* and *IL-6* pathways. Finally, short-term siRNA-based inhibition of mouse *Wrn* expression in the pre-adipocyte cell line 3T3-L1 confirmed the impact of *WRN* on adipogenesis. These results are consistent with the pro-inflammatory status and lipid abnormalities observed in WS patients. This approach thus identified new effectors of *WRN* activity that might contribute to the WS phenotype.

Introduction

Werner syndrome (WS) is a progeroid disorder that displays many of the clinical symptoms of normal aging at an early age.¹ Cells from WS patients have an elevated rate of spontaneous mutations and karyotypic abnormalities, in addition to aberrant

recombination, telomere defects, and hypersensitivity to agents that induce DNA damage and/or cellular stress. The *WRN* gene product, which is defective in WS, possesses helicase and exonuclease activities that are presumably important for preserving genome integrity.² *WRN* protein physically and functionally interacts with a number of enzymes that play pivotal roles in DNA replication and repair.³ These replication and recombination functions appear to also underlie telomere maintenance by RecQ helicases.^{3,4} Despite the advances in understanding how RecQ helicases contribute to DNA replication and repair, it is still unknown precisely how the absence of functional *WRN* leads to the numerous pathologies characteristic of Werner syndrome, some of which might be independent of genome maintenance defects (e.g., dyslipidemia and insulin resistance). Defects in transcription have also been observed in WS cell lines implicating *WRN* in some aspects of transcriptional control. For instance, nuclear extracts from WS lymphoblasts display a reduction in the transcription efficiency of a plasmid template bearing an RNA polymerase II-specific promoter compared to normal cells. The addition of normal cell extract or the addition of purified *WRN* protein can rescue transcription efficiency in this in vitro assay.⁵ A role for *WRN* in transcription is also suggested by the observation that overexpression of *WRN* results in enhanced p53-dependent transcriptional activity.⁶ Such observations indicate that *WRN* may affect RNA polymerase II transcription directly or indirectly.

The cDNA microarray is a powerful technique to look at the expression profile of thousands of genes in a given system. Such a technique has been utilized to compare the expression profile of primary human WS fibroblast cell lines with those derived from young or old normal donors.⁷ Transcription alterations in WS were strikingly similar to those in normal aging cells supporting the use of WS as an aging model and implying that the transcription alterations common to WS and normal aging represent general events in the aging process. However, one potential caveat is that fibroblasts derived from old donors or from WS patients also exhibit aneuploidy and chromosomal rearrangements.^{8,9} Such alterations

*Correspondence to: Michel Lebel; Centre de Recherche en Cancérologie; Hôpital Hôtel-Dieu de Québec; 9 McMahon St; Québec City, QC G1R 2J6 CA; Tel.: 418.691.5281; Fax: 418.691.5439; Email: michel.lebel@crhdq.ulaval.ca

Submitted: 04/06/09; Revised: 05/04/09; Accepted: 05/05/09

Previously published online as a *Cell Cycle* E-publication:
<http://www.landesbioscience.com/journals/cc/article/8925>

might affect gene expression in a fashion only indirectly related to the principal WS or age-related defects. In addition, *WRN* mutant cells may have undergone an adaptation process in vitro. To avoid these problems, we used short-term siRNA-based inhibition of *WRN* to test the consequences of WRN protein loss on gene expression in normal human diploid fibroblasts. Our findings indicate that WRN affects important pathways in lipidogenesis, adipocytes differentiation and inflammatory response in addition to those affecting DNA damage responses and cell cycle control. The results also indicate that a short-term knock down of WRN protein (only 48 hours after transfection of a small interference RNA against WRN mRNA) was sufficient to induce an expression profile resembling that of fibroblasts derived from old individuals.

Results

Gene expression analyses in WRN depleted normal human fibroblasts. Normal human diploid fibroblasts (GM08402) were transfected with a siRNA specific for WRN mRNA (referred as siWRN hereafter). Scrambled siRNA was used for control transfections. Based on the transfection protocol used with the Lipofectamine 2000 reagent, we determined that transfected cells reach full confluence 72 hours after transfection. The proliferation of GM08402 fibroblasts in culture is contact inhibited at confluence and this would interfere with gene expression and the interpretation of the data. To avoid this potential caveat, proteins and RNAs were extracted 48 hours after transfection of the siRNA molecules, at which point the cells had gone through only one population doubling. Transfection efficiency determined with an Alexa-488 labeled control siRNA (Qiagen Inc., Mississauga, ON) was more than 95%.¹⁰ To assess the efficiency of the siWRN-mediated knock down, WRN protein levels in transfected cells was examined by western blotting on total cell extracts. As indicated in Figure 1A, the most efficient knock down of WRN protein was achieved with HSS111385 siRNA (Invitrogen Inc., Burlington, ON) and corresponded approximately to a three-fold decrease compared to control siRNA transfection. Western blot analyses of shorter time points after transfection indicated WRN depletions less than 50% of control siRNA (Fig. 1A). We thus extracted cytoplasmic RNAs for microarray analyses 48 hours after transfection. Three independent transfection experiments (control siRNA and siWRN) were performed to extract cytoplasmic RNA. To determine the percentage of cycling cells 48 hours after transfection with control siRNA and HSS111385 siWRN, FACS analyses were performed. As indicated in Figure 1B, siWRN transfected cells showed an increase in the number of cells in G₁, from 71% to 77%, and a decrease in the number of cells in S-phase, from 28% to 18%, compared to siRNA control transfected fibroblasts. As WRN loss in cells is also associated with senescence, we measured the number of cells stained with the senescence-associated β -Galactosidase (SA- β -GAL)¹¹ in our transfected cells. As indicated in Figure 1C, there was approximately an 8% increase in the number of SA- β -GAL stained siWRN transfected cells compared to control transfected fibroblasts (48 hours after transfection). These results are consistent with the cell cycle data.

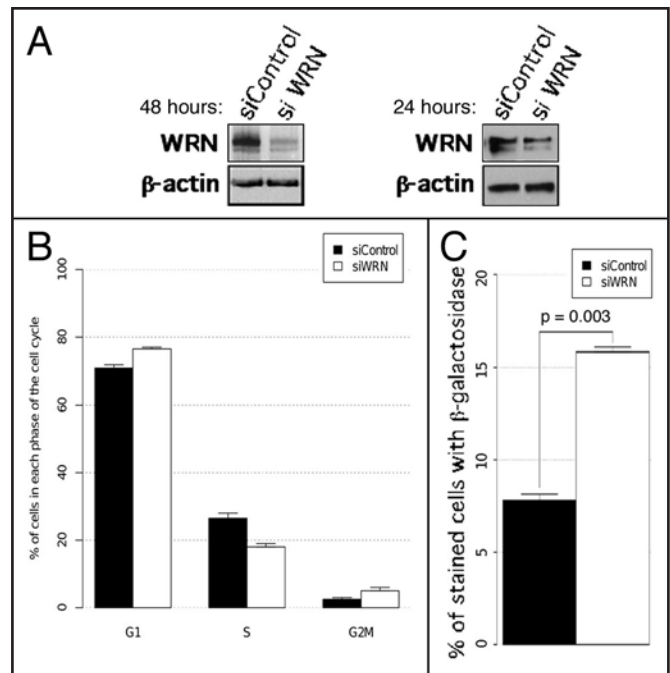


Figure 1. Impact of WRN protein expression on GM08402 diploid fibroblasts cell cycle 48 hours after transfection with scrambled siRNA and WRN specific siRNA. (A) WRN protein levels were revealed with an anti-WRN antibody by western blot 48 hours and 24 hours after transfection. The β -actin protein was used as control. (B) Percentage of cells in each phase of the cell cycle 48 hours after transfection with control siRNA and siWRN molecules determined by FACS analysis. Experiments were performed in duplicate. Bars represent the SEM. (C) Percentage of transfected cells stained for the senescence associated β -galactosidase. Bars represent the SEM. (t-test; p-value = 0.003).

Raw microarray data were normalized and a list of genes showing 1.5-fold difference in all three experiments with a False Discovery Rate (FDR) less than 0.1 in the siWRN transfected cells compared to siRNA control cells was generated. The cut off value of 1.5 was used to include genes that exhibited a subtle change in their expression due to a short-term WRN knock down. We found 660 genes exhibiting differential expression (118 and 542 genes were up and downregulated, respectively). The complete list of these genes can be found in Supplementary Table S1. To confirm the microarray data and the estimated FDR, western blot analyses were performed on a random set of 14 different proteins listed from the siWRN transfected GM08402 experiment (Suppl. Table S1). Western analyses were performed with antibodies against CCNB1 (cyclin B1), CDC2 (a cyclin-dependent protein kinase), FANCD2 (Fanconi anemia complementation group D2), FANCI (Fanconi anemia complementation group I), FANCI (Fanconi anemia complementation group J), FAS (a receptor involved in apoptosis signaling), HUWE1 (a ubiquitin-ligase), MRE11A, KIF4A (kinesin family member 4A), LMNA (lamin A/C), MAPK8 (mitogen-activated protein kinase 8), POLD1 (DNA polymerase δ sub-unit 1), SAFB1 (transcription factor), and TOP2A (topoisomerase II alpha). Nucleolin and β -actin, which are not present in our list of differentially regulated genes, were

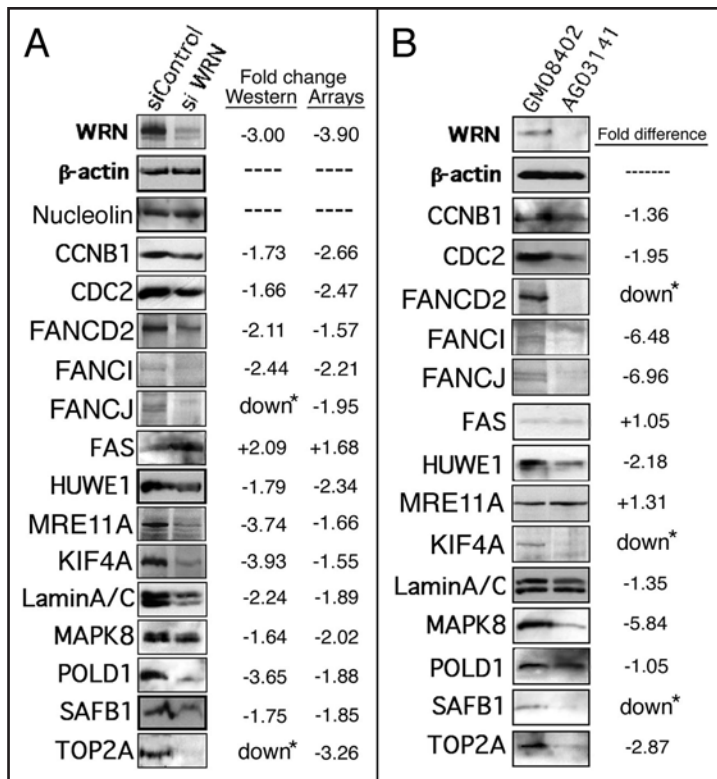


Figure 2. Protein expression levels in siWRN transfected and untransfected normal and WS fibroblasts. (A) Protein expression levels of 17 genes in normal human GM08402 diploid fibroblasts transfected with small interference RNA specific to WRN mRNA. These genes were selected randomly from the set of regulated loci. Scanning analyses of the western blots (from two independent experiments) are presented on the right of the blots. Data are expressed as the mean ratio of the indicated protein signals over the β -actin signal. The fold change in siWRN transfected cells is relative to cells transfected with scrambled siRNA (siControl). The fold change in mRNA expression based on the microarray analyses is also indicated. (B) Protein expression levels of 16 genes in WS AG03141 fibroblasts compared to normal human GM08402 diploid fibroblasts. Data are expressed as the mean ratio of the indicated protein signals over the β -actin signal. Asterisks indicate a qualitative estimation of the fold difference due to the low signal to high background ratio in some of the samples. All results are examples of blots from the same samples. Membranes were stripped and re-probed with the indicated specific antibodies.

used as controls. As indicated in Figure 2A, all the antibodies tested confirmed the upregulation or downregulation of these genes at the protein level following siWRN treatment. Interestingly, our preliminary microarray calculations indicated that nucleolin had a 2.6-fold decrease in expression with transfected siWRN molecules (data not shown). However, the calculated FDR for nucleolin based on the same microarray data was higher than 0.1 indicating a possible false positive. The western analysis of Figure 2A did not show difference at the protein level between control siRNA and siWRN transfection for nucleolin, thus supporting our analytical approach. In addition, duplication of quantitative RT-PCRs on total RNA extracted from control siRNA and siWRN transfected cells indicated no significant difference in nucleolin and β -actin mRNA levels between samples (data not shown) indicating that

it was indeed a false positive. Overall, the protein fold changes observed in our western blots were in good agreement with the predicted fold changes from the microarray data highlighted by a significant Pearson correlation of 0.68 (p-value = 0.008).

To confirm that this siWRN induced cellular state was maintained even in a cell line, we compared the expression levels of several proteins from our list in the WS cell AG03141 to untransfected GM08402 normal fibroblasts. As indicated in Figure 2B, several differences predicted from the siWRN experiments were observed, although for CCNB1, lamin A/C and POLD1 the differences in expression between AG03141 and GM08402 were small (less than 50% difference), while the other proteins exhibited more than 1.9-fold difference in expression. Thus, the expression of several proteins were also similarly altered in WS cells compared to siWRN transfected GM08402 fibroblasts. However, we did detect exceptions. MRE11A was increased in WS cells but significantly decreased in normal cells transfected with siWRN molecules. It is possible that a decrease in MRE11A in fibroblasts is potentially incompatible even with a slow cellular growth of WS cells in vitro, given the essential functions of MRE11 in promoting cell viability,¹² and WS cells with increased MRE11 expression may have been selected during growth in culture. POLD1 showed no significant difference in expression probably due to culture adaptation. Finally, FAS expression was too low to detect a clear difference between normal and WS fibroblasts. Thus, there were similarities but also differences between WS fibroblasts and cells with a short-term knock down of WRN.

Gene set enrichment analysis (GSEA). Classification of individual genes exhibiting at least a 1.5-fold difference in their expression (Suppl. Table S1) into specific gene ontologies indicated changes in four major classes of genes; those genes involved in signal transduction (during proliferation/differentiation), transcription, structural proteins and cell cycle control (Fig. 3A). To obtain an unbiased analysis of the genes up or downregulated by siWRN and more details on the exact biochemical pathways altered upon WRN depletion, we analyzed the complete list of genes using the Gene set enrichment analysis (GSEA) tool. GSEA is a way to assess if the expression of a predefined list of genes in a specific pathway is significantly modulated (either up or downregulated) under particular conditions (i.e., WRN knockdown). Such analysis was thus applied directly on the normalized data using the C2 curated gene set databases.¹³ Such databases contain gene sets from known pathways, expert-created pathways and also gene sets extracted from PubMed publications. The analysis generated a list of 57 significant gene sets with a False Discovery Rate (FDR) q-value below 0.05. Supplementary Table S2 shows in detail the gene enrichment sets down or upregulated in siWRN compared to control siRNA transfected cells. The complete GSEA reports are provided at http://www.crhdq.ulaval.ca/siWRN_GSEA. Overall, the 57 gene sets were classified into 14 biological pathways and are summarized in the histogram of Figure 3B. Findings included downregulation of genes known to be repressed in the p21/p53 pathway¹⁴ and in cell cycle progression pathways in multiple myeloma, in ductal

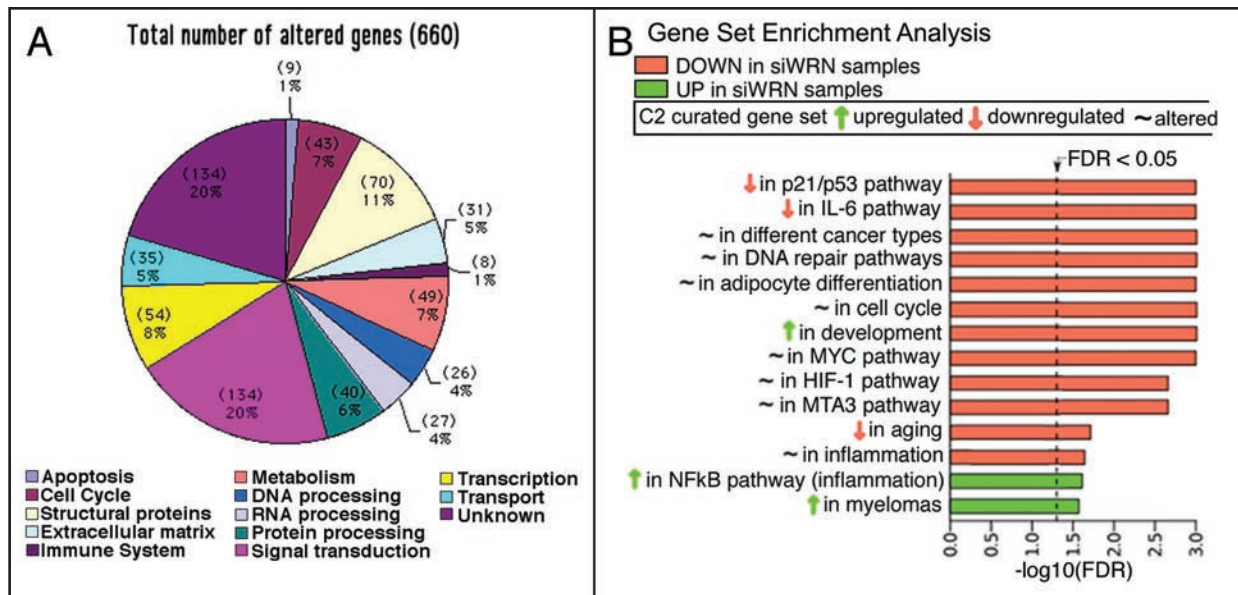


Figure 3. Classification and gene set enrichment analyses of expression data obtained from microarray experiments with WRN depleted fibroblasts. (A) Functional categories of genes exhibiting a 1.5-fold expression change in WRN depleted fibroblasts. The number of genes in each category and the percentages are indicated. (B) All significant gene set enrichments from human GM08402 normal diploid fibroblasts transfected with siWRN compared to control scrambled small interference RNA were grouped into biological and functional categories. Major categories with a FDR q-value less than 0.05 are presented in the histogram.

breast carcinoma, in proliferating and maturing B- or T-cells, and in fibroblasts responding to serum or to the proliferation induction of a virus.¹⁵⁻²³ The sets also included alteration of the E2F/Rb associated cell cycle pathway,^{24,25} the MYC pathway,²⁶⁻²⁸ the estrogen receptor regulation of proliferation in mammary epithelium via the transcription factor MTA3 pathway, and regulation of pre-B lymphocyte proliferation via the cellular E2A transcription factor pathway.²⁹ Genotoxic response pathways to different drugs including cisplatin and the topoisomerase II inhibitor etoposide were downregulated as well (including ATR-BRCA1/2 pathway in response to DNA damage).³⁰⁻³⁵ Pathways affecting tumor progression in different cancer types including non-BRCA1/2 breast cancer types were also altered by siWRN.^{13,36-40} Pathways involved in adipocyte differentiation were also downregulated significantly.⁴¹⁻⁴³ The siWRN affected the transcription factor ETV5 pathway and different aspects of neuro-development.⁴⁴⁻⁴⁶ There was a significant overlap between sets of genes associated with fibroblasts derived from elderly individuals or derived from progeria patients⁴⁷ and short-term WRN depleted fibroblasts. Finally, the genes known to be downregulated in the IL-6 response pathway and the HIF-1 pathway were also downregulated in siWRN transfected cells.⁴⁸ Two pathways related to inflammatory signaling were upregulated, namely the NFκB transcription factor activated pathway⁴⁹ and genes associated with interferon response in neutrophils.⁵⁰ The siWRN also overlapped significantly with a set of interferon responding genes downregulated during cytomegalovirus infection⁵¹ (Suppl. Table S2). Thus, our findings indicate that WRN affects important pathways in lipidogenesis, adipocytes differentiation and inflammation in addition to those affecting DNA damage responses and cell cycle control. The results also indicate that a short-term knock down of WRN protein (only 48

hours) was sufficient to induce an expression profile resembling that of fibroblasts derived from old individuals.

Motif gene set enrichment analysis for transcription factors in WRN depleted fibroblasts. We next performed GSEA directly on the normalized data using the C3 motif gene set databases. This tool allows the identification of gene sets that contain genes sharing a cis-regulatory motif that is conserved across the human, mouse, rat and dog genomes.⁵² The complete GSEA reports for motif sets are provided at http://www.crhdq.ulaval.ca/siWRN_GSEA. No significant common motif was detected for genes upregulated by the siWRN molecules. In contrast, 22 transcription factor binding sites shared among genes that were downregulated in siWRN transfected cells were identified with an FDR q-value below 0.05 (Table 1). The highest significant scores were obtained with motifs recognized by E2F family members. This finding is consistent with the result obtained with the GSEA on the C2 curated gene set databases (downregulation of the E2F1, pRB/E2F and cell cycle pathways) and the significant downregulation of E2F2 and E2F8 expression in the microarray data (Suppl. Table S1). The second transcription factor binding site identified as shared by many promoters was the MYC associated factor X or MAX (Table 1). Accordingly, the MYC pathway was downregulated in siWRN transfected cells (Suppl. Table S2).

WRN pathway network mapping in WRN depleted fibroblasts. The Ingenuity Pathways Analysis (IPA) software is another powerful complementary tool to identify and visualize biochemical and/or biological networks associated with WRN depletion in cells. It allows us to compare co-expression interactions with interaction information that was manually curated from the literature and to annotate these interactions with the closest matching biological functions. For this analysis, we focussed on our lists of

Table 1 Promoter motif set analyses from siWRN transfected GM08402 fibroblasts

Transcription factors		FDR
1. E2F family members	(including E2F, E2F1, E2F4, DP-1, DP-2)	<0.001
2. MAX	(MYC associated factor X)	0.003
3. NF- μ E1	(nuclear factor interacting with the immunoglobulin enhancer element)	0.005
4. ARNT	(aryl hydrocarbon receptor nuclear translocator)	0.008
5. REBP1	(sterol regulatory element binding transcription factor 1)	0.009
6. NF-Y	(also known as CCAAT-binding factor)	0.011
7. USF	(upstream regulatory factor 1)	0.012
8. YY1	(Yin and Yang 1 nuclear factor)	0.014
9. SP1	(Simian-virus-40 protein 1)	0.015
10. GATA2	(GATA binding protein 2)	0.018
11. GABP	(GA binding protein transcription factor, beta, sub-unit 2)	0.020
12. MAZ	(MYC associated zinc finger protein; purine-binding factor 1)	0.026
13. PAX4	(paired box gene 4)	0.029
14. STAT1	(signal transducer and activator of transcription 1)	0.030
15. SOX-9	(sex determining region Y-box 9)	0.034
16. ELK1	(member of ETS oncogene family)	0.035
17. C-MYB	(myeloblastosis viral oncogene homolog, avian)	0.035
18. SRF	(serum response factor; c-fos serum response element binding factor)	0.035
19. ZIC3	(Zic family member 3 heterotaxy 1; odd-paired homolog, Drosophila)	0.035
20. NRF-1	(nuclear respiratory factor 1)	0.036
21. OCT1	(Pou domain, class 2, transcription factor 1)	0.038
22. SMAD1	(mothers against DPP1 homolog 1, Drosophila)	0.037

Do not distribute.

genes exhibiting a 1.5-fold difference in their expression (Suppl. Table S1). The analysis of the data confirmed the involvement of WRN in cell cycle and DNA replication/repair networks (Fig. 4). In addition, the IPA confirmed the up and downregulation of sets of proteins involved in lipid metabolism. For better visualization, the WRN protein-containing network in Figure 4 was merged to the lipid metabolic network (Fig. 5A). The IPA also revealed a gene set involved in inflammatory responses. The WRN protein-containing network in Figure 4 was merged to the inflammatory responses network for better visualization (Fig. 5B). Interestingly, the top five significant networks affected by WRN depletion revealed by IPA included DNA replication and cell cycle, cytotoxic stress response, DNA recombination and repair, cellular transformation (cancer) and neurological diseases (data not shown).

Concordance of siWRN-related gene expression changes to other global expression studies on aging. We compared our lists of genes altered by siWRN with several published lists of genes whose expression was altered in young vs. old fibroblasts as well as in Gilford-Hutchinson and Werner expression profile studies.^{7,47} As indicated in Supplementary Table S2, the GSEA indicated a significant overlap between the list of genes downregulated in fibroblasts derived from old individuals compared to young individuals⁴⁶ and the list of genes downregulated in our siWRN experiments. Similarly, there is a significant overlap in the number of downregulated genes in the siWRN list and the Gilford-Hutchinson microarray data from the same study.⁴⁶ We then compared our data to the landmark study indicating that transcription

alterations in WS are strikingly similar to those in normal aging cells.⁷ Unfortunately, proper comparison could not be performed as the array used in their study and our analysis contained few common genes. Only 3,685 genes were present in both Kyng and colleagues' microarray⁷ and our Agilent microarray (Suppl. Fig. S1). Thirty-eight percent of the genes listed in Supplementary Table S1 are present in the microarray used by Kyng et al.⁷ Only ten genes exhibited at least a 1.5-fold expression difference in both studies (Fig. S1B and C). Nonetheless, the fact that siWRN data overlapped significantly with the old versus young study raises the possibility that transient loss of WRN induces a cellular state that immediately resembles that of aging.

Concordance of siWRN-related gene expression changes to Wrn mutant mouse studies. We compared our results with data generated by comparing mouse embryonic cells with a deletion in the helicase domain of the murine *Wrn* protein to wild type mouse embryonic cells.⁵³ For our comparison, we first generated a list of mouse orthologous genes (genes present in both the human and mouse microarrays) exhibiting at least a 1.5-fold expression differences between wild type and *Wrn* mutant mouse embryonic fibroblasts. Although the mouse embryonic cell population established from such helicase mutant *Wrn* mice comes from different embryonic tissues compared to human GM08402 cells which were derived specifically from skin fibroblasts, 87 orthologous genes showed similar changes between human GM08402 fibroblasts transfected with siWRN molecules and mouse embryonic cells established from *Wrn* helicase mutant animals (Fig. 6A). Statistical

Effect of short-term depletion of WRN protein

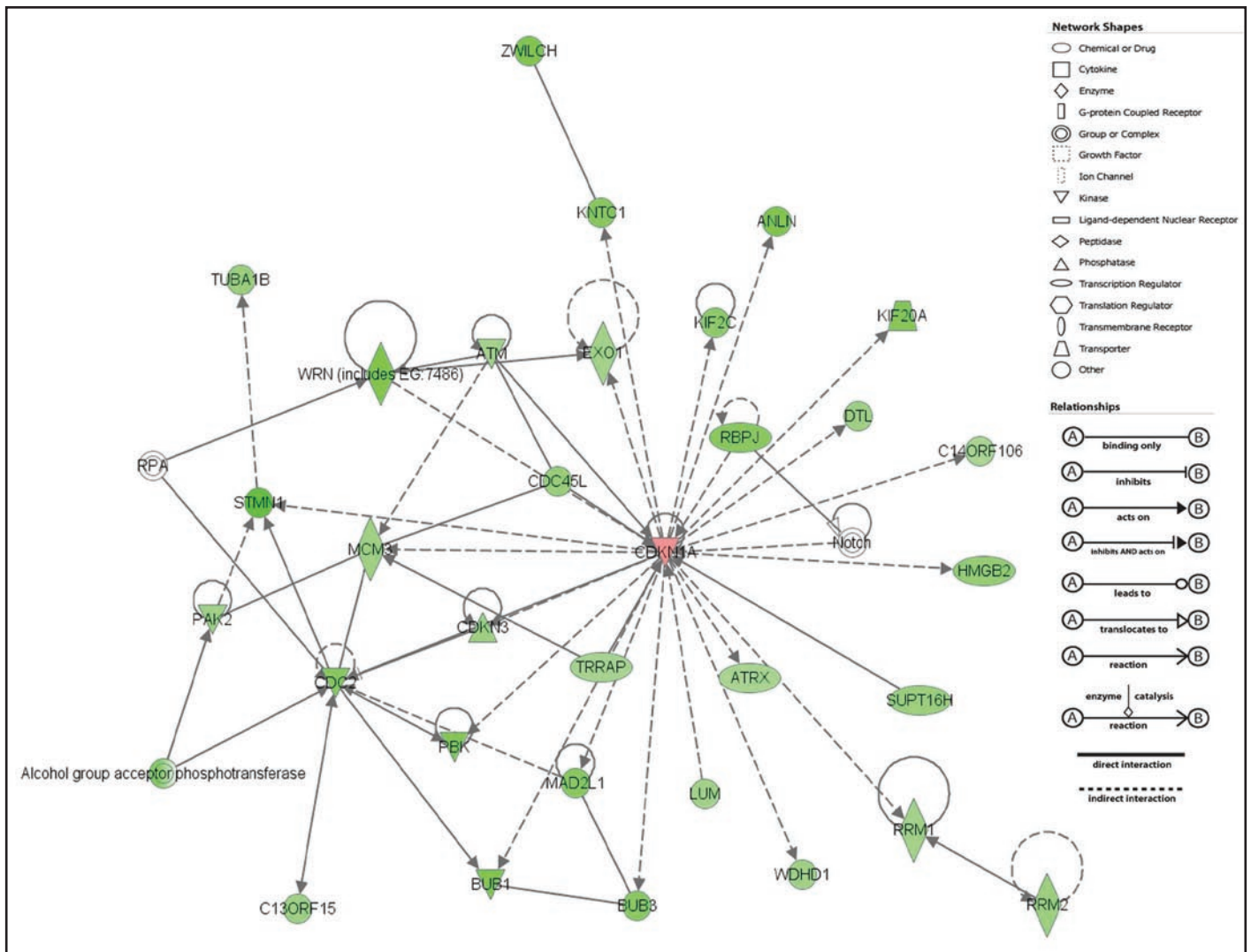


Figure 4. WRN network representation using the Ingenuity Pathways Analysis of WRN depleted human normal fibroblasts. The networks are based on the list of genes exhibiting at least a 1.5-fold change in expression. The legend on the right provides a key of the main features of Network Explorer including molecule shapes and colors as well as relationship labels and types. Molecules in red are upregulated [has a positive (+) expression value]. Molecules in green are downregulated [has a negative (-) expression value]. Molecule in white are not present in our list of genes exhibiting 1.5-fold change in expression, but are incorporated into the network through relationships with other molecules.

analyses indicated a significant overlap (p -value = 0.0078) between the human WRN depleted cells and the *Wrn* mutant embryonic fibroblasts (see Suppl. Fig. S2 for details of the statistical analysis). GSEA on cytoplasmic RNA extracted from mutant *Wrn* helicase embryonic cells⁵³ (GEO data sets GSE3359 at <http://www.ncbi.nlm.nih.gov/geo/>) were performed to obtain more details on the pathways affected in *Wrn* mutant fibroblasts. Such GSEA indicated significant enrichment of downregulated gene sets associated with DNA repair³⁰ and cell cycle.¹⁵⁻¹⁹ Other sets of genes involved in proliferation (cell cycle) were upregulated in embryonic mouse cells. Concomitantly, genes associated with transformation of different cancer types including multiple myelomas³⁹ were upregulated in these mouse cells as well. The IL-6 pathway was upregulated.⁴⁸ Finally, genes known to be upregulated and downregulation during adipocyte differentiation⁴¹ were respectively down and upregulated in *Wrn* mutant mouse embryonic cells indicating inhibition in

this biological process. Thus, nine biological processes or pathways were overlapping with the 14 pathways significantly altered in siWRN transfected human cells (compare Figs. 3B and 6B).

Short-term siRNA-based inhibition of mouse *Wrn* expression in the pre-adipocyte cell line 3T3-L1. To confirm the impact of WRN protein levels on adipogenesis, we transfected the murine pre-adipocyte cell line 3T3-L1 with siRNA against mouse *Wrn* mRNA (referred as siWRN hereafter). The 3T3-L1 cell line forms a unique system for the analysis of adipocyte differentiation in vitro. Scrambled siRNA was used for control transfections. Transfection was performed on confluent cultures 24 hours before the induction with appropriate factors in the media. To estimate the efficiency of the transfection, whole cell extracts were analyzed by western blotting with an antibody against mouse *Wrn* protein after transfection from day zero to day five during the differentiation process. As indicated in Figure 7A, the level of mouse *Wrn*

Effect of short-term depletion of WRN protein

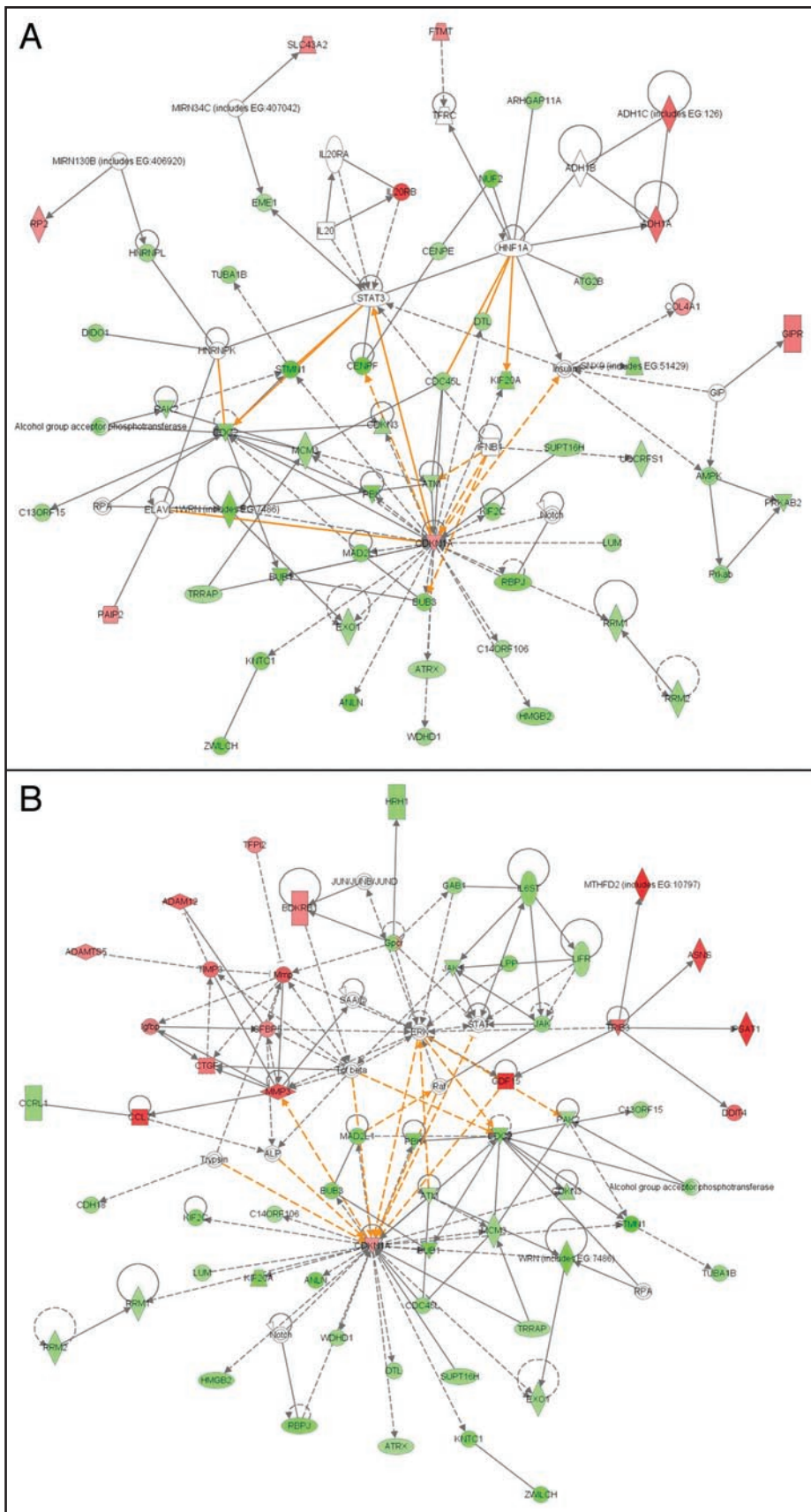


Figure 5. Representation of the lipid metabolism network and the inflammatory response network merged to the WRN protein-containing network using the Ingenuity Pathways Analysis software. The networks are based on the list of genes exhibiting at least a 1.5-fold change in expression 48 hours after siWRN transfection. (A) Merged WRN and lipid metabolism networks in WRN depleted cells. Molecules in red are upregulated [has a positive (+) expression value]. Molecules in green are downregulated [has a negative (-) expression value]. Molecule in white are not present in our list of genes exhibiting 1.5-fold change in expression, but are incorporated into the network through relationships with other molecules. Colored lines in the figures represent overlapping biochemical paths. (B) Merged WRN and inflammatory response networks in WRN depleted cells.

protein was decreased by approximately two- to four-fold from day one to day three during the differentiation process. The expression of adipogenesis markers like the transcription factor *C/EBPβ* and fatty acid synthase (*FASN*) was also examined on the same blots. Expression of *C/EBPβ* increased at the third day of differentiation in control transfected cells (Fig. 7A). The expression of *C/EBPβ* was 20–24% lower in siW_{rn} transfected cells by the fourth and fifth days of differentiation compared to control siRNA (Fig. 7B). Similarly the expression of *FASN* was 12–30% lower in siW_{rn} transfected cells from day two to four during the differentiation process compared to 3T3-L1 cells transfected with the control siRNA (Fig. 7C). Protein expression of fatty acid synthase picked up after five days of differentiation, which corresponded to the decrease in siWRN, knock down effect in 3T3-L1 cells. At the end of the differentiation protocol, the differentiation of transfected 3T3-L1 adipocytes was estimated with Oil Red O, a standard staining procedure for lipidogenesis and thus adipogenesis.^{41,42} As seen in Figure 7D, there was a significant 14% decrease in lipid production in cells transfected with the siW_{rn} compared to cells transfected with the control siRNA molecules. Re-transfection of 3T3-L1 with siW_{rn} molecules during the differentiation period (at day 5 for example) caused cells to detach from the dishes and die preventing any measurements. Despite such limitations of this system, the results indicate that a transient knock down of mouse W_{rn} protein is sufficient to affect lipidogenesis or adipogenesis

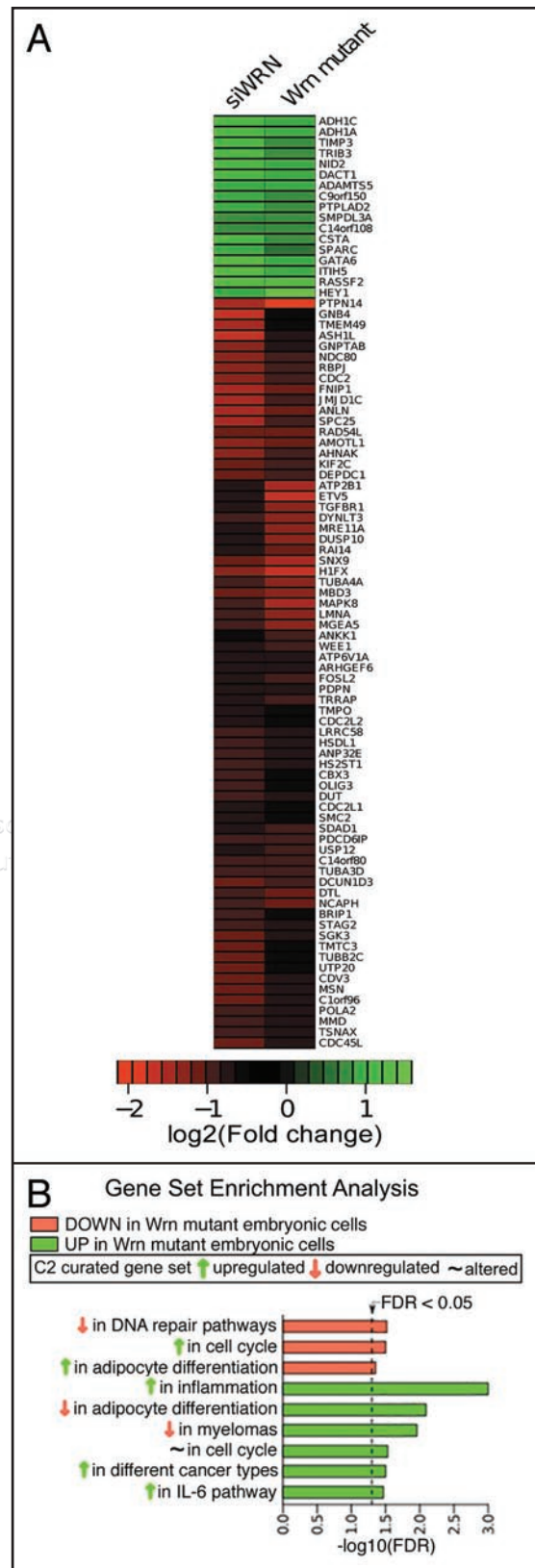
Figure 6. Comparison of microarray data between GM08402 diploid fibroblasts transfected with small interference RNA specific to WRN and mouse embryonic cells established from *Wrn* helicase mutant animals. (A) List of genes similarly changed between siWRN transfected human fibroblasts and *Wrn* helicase mutant embryonic cells. (B) Gene set enrichments from *Wrn* helicase mutant embryonic cells compared to wild type cells (GEO data sets GSE3359 at <http://www.ncbi.nlm.nih.gov/geo/>) grouped into biological and functional categories. Major categories with a FDR q-value less than 0.05 are presented in the histogram.

in vitro. Moreover, the short-term *Wrn* knock down result with the 3T3-L1 is in agreement with the GSEA findings with WRN depleted human cells.

Discussion

Telomere defects and the other forms of genome instability observed in WS fibroblasts are thought to contribute to the premature senescence of these cells. However, it is possible that the absence of WRN has important effects on gene expression^{5,6} that might be independent of genome instability and also contribute to cell senescence or other aspects of premature aging in WS. To avoid accumulation of mutations that could affect transcription indirectly, we used siRNA to specifically reduce expression of WRN for only 48 hours in culture. Small interference RNAs were used in this study instead of shRNAs or strategies using retroviral vectors, to specifically target WRN mRNA directly without the requirement for cellular RNA synthesis or selection with resistance markers that could potentially affect the outcome of the expression profile. In our experience, transfection efficiency with siRNA molecules is more than 90%. Several siWRN molecules were tried and the best knock down achievable 48 hours after transfection was approximately a three-fold decrease compared to control siRNA. We extracted cytoplasmic RNA only after 48 hours to avoid altered gene expression due to contact inhibition at confluence (72 hours after transfection). Shorter time points were not included in this study as WRN depletion was less than 50% of wild type. Although with a 48 hours knock down time frame we did not achieve 100% WRN protein depletion in human fibroblasts, our list of genes in all three biological replicates overlapped significantly with sets of genes recovered from old age fibroblasts vs. young age fibroblasts and progeria derived fibroblasts vs. normal donor fibroblasts.⁴⁷ In addition, the increase in the senescence associated β -galactosidase in WRN depleted cells is consistent with the GSEA. These results thus confirmed the conclusion drawn by Bohr and colleagues⁷ that WRN deficient cells exhibit a phenotype resembling cells derived from old donors. We did detect differences, however, regarding the expression of some proteins by western blots between WS cells derived from patients and WRN depleted cells for 48 hours. There are several possibilities potentially explaining these differences. One obvious possibility is the karyotype and the accumulation of mutations suspected to occur in WS cell might interfere with the expression of several genes. Another possibility is a cellular adaptation of WS cells to culture conditions that could influence gene expression. Nevertheless, GSEA analyses did show significant overlap between old age fibroblasts and WRN depleted cells in our study.

The overlap with Hutchinson-Gilford progeria syndrome (HGPS) is interesting as siWRN decreased the expression levels of



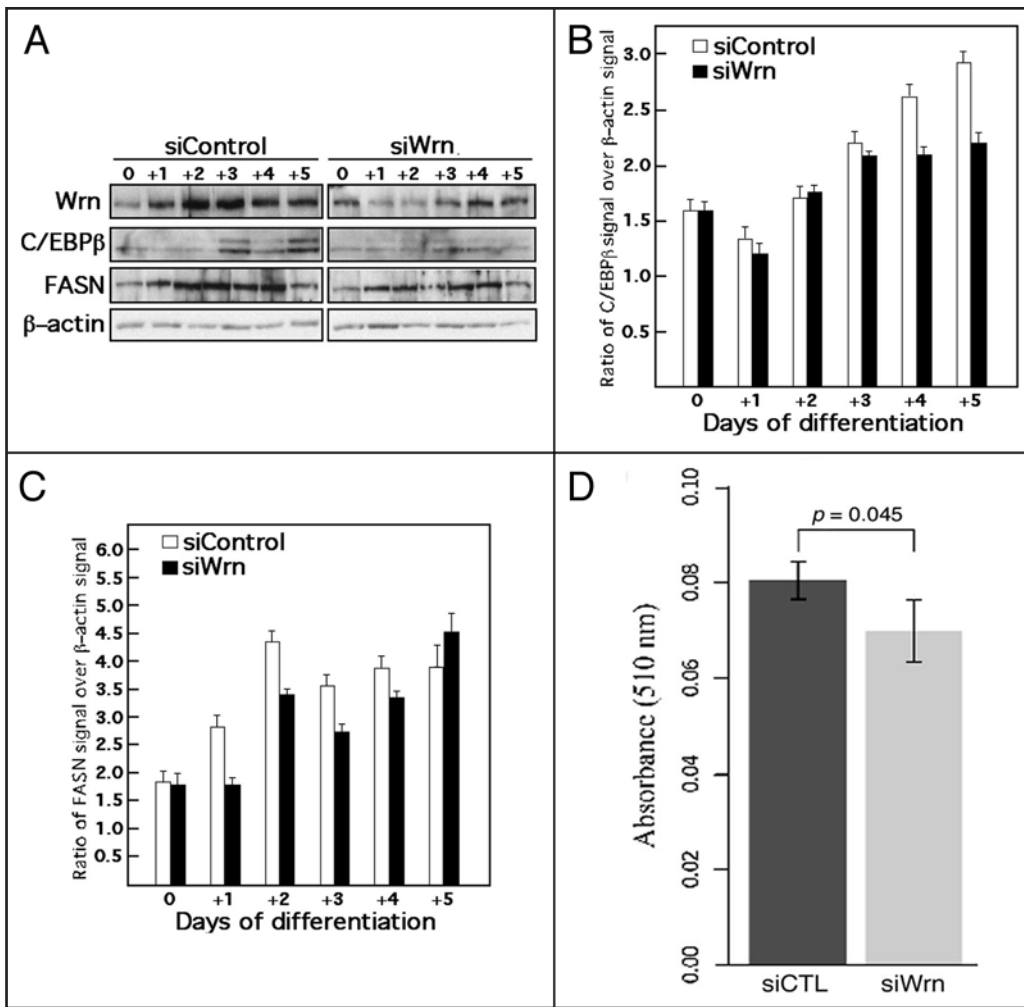


Figure 7. Mouse Wrn, C/EBPβ and fatty acid synthase protein levels in 3T3-L1 pre-adipocytes at different time points after adipogenesis induction. (A) Example of western blots showing Wrn, C/EBPβ and fatty acid synthase (FASN) protein levels. The β-actin protein present in the lysates was used as control. Time zero corresponds to the addition of the differentiation factors in the culture media. Cells were transfected with the indicated siRNA molecules 24 hours before the addition of the differentiation cocktail. The experiments were repeated twice. (B) Scanning analyses of the western blots expressed as the ratio of C/EBPβ signal to β-actin signal in transfected cells. Bars represent the SEM. (C) Scanning analyses of the western blots expressed as the ratio of fatty acid synthase (FAS) signal to β-actin signal in transfected cells. Bars represent the SEM. (D) Lipid amount in cells detected by Oil Red O staining in control (siCTL) and siWrn transfected cells at the eighth day of differentiation. Oil red O (maker of adipogenesis) released from transfected cells was measured with a spectrophotometer at 510 nm. Experiments were performed twice, each time in triplicate. Bars represents the SEM. (*p*-value was calculated with an unpaired *t*-test).

lamin A (LMNA), the gene responsible of the pathology observed in this syndrome (at least in a subset of LMNA mutations).⁵⁴ Although HGPS is caused by a dominant mutation in LMNA, decreased Lamin A/C protein levels as seen in our WRN depleted fibroblasts should affect the nuclear envelop of cells. Accordingly, WS fibroblasts are known to exhibit abnormal overall nuclear morphology.⁵⁵

We do not expect that all the 660 genes exhibiting a decrease at the mRNA level will translate into decreased protein levels, even though based on the 14 randomly picked genes, our western blots confirmed the microarray data with a Pearson

correlation of 0.68 (*p*-value = 0.008). Our data points to sets of genes that potentially would have an impact on certain aspect of WS or aging in general. For example, much attention has been focused on the roles of WRN in DNA repair and cell cycle checkpoints.³ Consistent with these roles, we observed changes in the expression of genes involved in DNA replication and DNA repair (Suppl. Table S2). In addition, several important pathways related to cell cycle were detected by gene set enrichment analysis (GSEA) in siWRN transfected cells. These include the p53/p21 pathway as well as targets of the E2F, MTA3, cellular E2A, and the MYC transcription factor pathways during cell cycle. The interaction of WRN with p53 and its impact on p21 expression and attenuation of apoptosis is well described in the literature.^{6,56,57} It has been established that MYC stimulates the transcription of WRN.⁵⁸ We did not see changes in MYC expression in our depleted WRN fibroblasts based on our microarray data. However, the MYC response pathway is downregulated in siWRN transfected cells based on GSEA. Overexpression of MYC was previously found to induce cellular senescence in WRN depleted cells,⁵⁸ and therefore the downregulation of the MYC response pathway might reflect a compensatory response to the loss of WRN

that enables continued cell growth. Moreover, we observed changes in the expression of the MYC binding protein (MYCBP) and HUWE1, an ubiquitin-ligase which affects the transcriptional activity of MYC.⁵⁹ Overall, these results indicate an obvious impact on cell proliferation consistent with the decrease in the number of cells in S phase observed after our transfection with siWRN molecules. Furthermore, the GSEA showed a decrease in genes involved in DNA replication (Suppl. Table S2). The GSEA also indicated downregulation of genes involved in progression of several tumor types (Suppl. Table S2). Noticeably, recent data with siWRN transfected tumor cells revealed that the inhibition

of WRN expression strongly impairs growth of several cancer cell lines in mouse xenograft models.⁶⁰

In addition to cell cycle pathway defects, siWRN transfected cells exhibited impairment of a response pathway common to several genotoxins including cisplatin, doxorubicin, 5-fluorouracil, methyl methanesulfonate, mitomycin C, taxol, hydroxyurea and etoposide.^{30,31} Although WRN mutant cells respond differently to these agents, the defect in DNA damage response predicted from our observations, even in the absence of treatment, is consistent with the results obtained by Kyng and colleagues.⁶¹ We also observed a significant overlap between a set of siWRN downregulated genes and the ATR-BRCA1 pathway (Suppl. Table S2). Accordingly, there is evidence for collaboration between BRCA1 and WRN during cellular responses to DNA inter-strand cross-links.⁶² One possibility is that a BRCA1/WRN complex may also affect the regulation of a specific set of genes at the transcriptional level.

Interestingly, the GSEA indicated alterations in genes involved in brain development (Suppl. Table S2). Furthermore, the IPA also revealed neurological diseases as one of the protein networks affected by a 48 hours knock down of WRN protein. Although neurodegenerative disease is not a major phenotype associated with WS, there are a number of studies reporting neurological pathologies associated with several WS patients.⁶³⁻⁶⁵ Thus, the GSEA and the Ingenuity Pathway analysis (IPA) are two independent tools for data integration and visualization that provided converging results. They complemented each other and delivered a more detailed view of the biological network affected by a WRN knock down.

The siWRN transfected cells displayed apparent impairment of adipocyte differentiation pathways. Importantly, the impact of the mouse WRN homologue (knock down of *Wrn* mRNA) on lipogenesis was confirmed in mouse 3T3-L1 pre-adipocytes (Fig. 7). Although the knock down of mouse *Wrn* was not 100% efficient, our experimental setting was sufficient to show an effect on C/EBP β and fatty acid synthase expression, and lipid accumulation in 3T3-L1 cells during differentiation. The overall effect on lipid accumulation was only approximately 16% less than the control. Nevertheless, our results points to a role for WRN in adipocyte differentiation and is consistent with the loss of subcutaneous fat observed in WS patients.⁶⁶ However, it is noteworthy that WS patients often have high levels of visceral fat, indicating that loss of WRN does not prevent adipogenesis in all cell types. Our results also point to the limit of working with adipocytes in vitro in the absence, for example, of adipokines normally secreted into the circulation by the liver to maintain lipid homeostasis. Interestingly, the GSEA indicated that several genes involved in cell cycle during adipocyte differentiation were downregulated. This indicates that not only differentiation of adipocytes may be affected in vivo, but possibly proliferation as well.

Also of interest, siWRN transfected cells also exhibited changes in HIF-1, IL-6 and NF κ B response pathways that overall indicate a pro-inflammatory pattern. These findings support the concept of "inflamm-aging" put forward by Davis and Kipling as an important aspect of the WS phenotype.⁶⁷ Recent data on fibroblasts derived from WS patients have shown activated molecular pathways

involved in inflammation.⁶⁷ This is consistent with the presence of high plasma levels of inflammatory cytokines like IL-6 in WS individuals. With regard to NF κ B, this transcription factor determines cell response to a wide variety of stresses including inflammation and was recently shown to be one of the most strongly age-associated markers.⁶⁸ The RNA levels of NF κ B did not fluctuate in siWRN transfected cells. However, it is known that the NF κ B pathway can be modulated through NF κ B phosphorylation. Our results are consistent with recent results obtained on mice bearing a deletion of the *Wrn* helicase domain. We observed an increase in NF κ B phosphorylation and activation in such *Wrn* mutant mice compared to wild type animals (manuscript submitted), indicating upregulation of NF κ B pathways may be a conserved feature of the WS phenotype.

Finally, emphasize that we do not yet know the mechanisms by which decreased levels of WRN affect transcription. It is conceivable that WRN might associate with chromatin and affect the activity of classical transcription factors, or that it might affect chromatin structure directly by unwinding DNA secondary structures or by regulating DNA supercoiling through its interaction with topoisomerase I.^{10,69} Additional studies will be required to investigate these possibilities. Nonetheless, our findings provide novel avenues of research in the field of WS.

Materials and Methods

Cells. The normal human fibroblast primary cell strain (GM08402 passages 8–15) and the human Werner syndrome fibroblast primary cell strains (AG03141 passage 12) were obtained from the Coriell Cell Repositories (Camden, NJ) and were maintained in DMEM with 50 μ g/mL streptomycin and 10% fetal bovine serum. Mouse 3T3-L1 cells were purchased from the American Type Culture Collection. They were grown in DMEM medium (4,500 mg/L glucose) supplemented with 10% FBS. Two days after reaching confluence, cells were first incubated with adipogenesis induction media (basal media containing 250 μ M IBMX, 250 nM dexamethazone, and 5 μ g/mL insulin) for 48 hours after which they were maintained in media containing only insulin (5 μ g/mL) for four additional days. Lastly, fresh media without insulin, IBMX and dexamethazone was added to the differentiating cells for a final 48 hours.

Transfection of small interference RNAs and plasmids. Stealth small interference RNAs specific for WRN mRNA were purchased from Invitrogen Inc., (Burlington, ON). The sequences are (coding strand) 5'-UUA ACC AGA CUG UUA AGG CUC CAG G-3' (HSS111385); 5'-UUU CGA ACU AGG CAG AAG AAA CUU C-3' (HSS111386); and 5'-AUU AUA ACA AUG CUC UUU GGU GCC C-3'. (HSS111387) for WRN mRNA. The siRNA HSS111385 gave the best knock down of WRN protein levels and was used for the microarray experiments. Cells were transfected with siRNAs using Lipofectamine 2000 reagent (Invitrogen Inc., Burlington, ON) according to the manufacturer's instructions to knock down WRN protein levels. Transfected cells were incubated at 37°C for 48 h. Transfection efficiency was determined with an Alexa-488 labeled control siRNA (Qiagen Inc., Mississauga, ON). The knock down efficiency was confirmed by western blot

analyses. Mouse 3T3-L1 cells were transfected with a Stealth small interference RNAs specific for mouse *Wrn* (MSS212619 coding strand; 5'-CCU CUG UUG GGA GUC AUC AAA CAU U-3') using Lipofectamine 2000 reagent on confluent cultures 24 hours before the induction of adipocyte differentiation with appropriate factors.

FACS analyses. The normal fibroblast primary cell strain (GM08402) were transfected using the Lipofectamine 2000 reagent (Invitrogen Inc., Burlington, ON). Forty-eight hours later, cells were fixed in 50% ethanol overnight at 4°C. Cells were then washed in PBS and incubated for 30 min at 37°C in a buffer containing propidium iodide and RNases. Cell cycle analyses were performed on a Beckman-Coulter Epics Elite ESP (Cambridge, MA) flow activated cell sorter. Data were analyzed with the MultiCycle software (Phoenix Flow System, San Diego, CA).

Senescence associated β -galactosidase staining. Senescence-associated β -galactosidase (SA- β -Gal) was used as a marker of senescence, and cells were stained for this marker as described.⁷⁰ The percentage of blue SA- β -Gal positive cells was determined by counting, in 4 different fields, at least 200 cells (inverted microscope Nikon TMS).

Microarray analysis. RNAs from the control, siWRN transfected cells were extracted according to Sambrook et al.⁷¹ and labeled with Cyanin-3 or -5 labeled CTP (PerkinElmer, Boston, MA). Labeled cRNAs were purified using the RNeasy Mini kit (Qiagen, Mississauga, ON) and were hybridized onto human Agilent 60-mer Oligo Microarrays (44,000 genes/microarray) in triplicates using the in situ Hybridization Plus kit (Agilent, Palo Alto, CA) following the manufacturer's instructions. Arrays were scanned using a dual-laser DNA microarray scanner. To generate a list of selected genes, microarray data extracted from images by the Feature Extraction software 6.1 (Agilent, Palo Alto, CA) were analyzed using GeneSpring software. Briefly, the background signal was subtracted and data were normalized using Lowess normalization to correct for artifacts caused by inconsistencies of the relative fluorescence intensity between some red and green dyes. This was followed by filtering on an expression level greater than 1.5-fold in all three independent transfection experiments. The p-values coming from an unpaired t-test were adjusted using the Benjamini-Hochberg method, across all genes and all comparisons, to control the expected false discovery rate (FDR) at less than 10%.⁷²

Gene set enrichment analysis. Gene set enrichment analysis (GSEA) was applied using default parameters on a fold change sorted list of genes on the C2 curated gene sets database.¹³ Such databases contain gene sets from known pathways, expert-created pathways and also gene sets extracted from PubMed publications. Gene enrichments were considered significant with a False Discovery Rate (FDR) q-value below 0.05.

Ingenuity pathways analysis. Ingenuity Pathways Analysis (IPA) software (<http://www.ingenuity.com>) allowed us to compare co-expression interactions with interaction information that was manually curated from the literature and to annotate these interactions with the closest matching biological functions. The user-input or "focus" gene list was compared to the "Global Molecular Network" (GMN) database consisting of thousands

of genes and interactions. The focus genes were sorted based on highest to lowest connectivity within the GMN, and then networks of approximately 35 genes were grown starting with the most connected focus gene. IPA creates networks based on the principle that highly connected gene networks are most biologically meaningful. It assigns a p-value for a network of size *n* and an input focus gene list of size *f* by calculating the probability of finding *f* or more focus genes in a randomly selected set of *n* genes from the GMN. The IPA interaction database is manually curated by scientists and updated quarterly.

Western blots. All transfected and untransfected cells were lysed in RIPA buffer [50 mM Tris-HCl (pH 7.5), 150 mM NaCl, 1% NP-40, 0.1% SDS, 0.5% sodium deoxycholate] for SDS-PAGE analyses. Proteins from SDS-PAGE were transferred onto Amersham Hybond-P membranes (GE Healthcare Limited, Piscataway, NJ). Membranes were blocked two hours at room temperature in PBS containing 5% milk/0.1% Tween, washed in PBS-Tween (0.1%), and incubated overnight with the primary antibodies in PBS containing 5% milk overnight at 4°C. Blots were washed the next day in PBS-Tween and incubated two hours at room temperature with horseradish peroxidase-conjugated secondary antibody in PBS containing 5% milk. Blots were washed with PBS-Tween and proteins were revealed with chemiluminescence reagents (ECL Plus; GE Healthcare Limited, Piscataway, NJ). The human WRN protein was detected with an anti-WRN polyclonal antibody from US Biologicals (Swampscott, MA). The polyclonal antibody against mouse *Wrn* protein (H-300) was purchased from Santa Cruz Biotechnology (Santa Cruz, CA). The other antibodies used in this report are the anti-cyclin B1 monoclonal antibody (Cell Signaling Technology, Inc., Danvers, MA), the anti-Topoisomerase II α monoclonal antibody and the anti-CDC2 monoclonal antibody (US Biologicals, Swampscott, MA), the anti-SAFB monoclonal antibody and the anti-FAS monoclonal antibody (Upstate Biotechnology, Lake Placid, NY), the anti-MAPK8 rabbit polyclonal antibody (AbCam, Cambridge, MA), the anti- β -actin monoclonal antibody (Sigma-Aldrich, St. Louis, MI), the anti-DNA polymerase delta-1 monoclonal antibody (BD Biosciences, Palo Alto, CA), the rabbit polyclonal antibody against FANCD2 and the mouse monoclonal antibody against FANCI (Novus Biologicals, Littleton, CO), the rabbit polyclonal antibody against FANCI and the rabbit polyclonal antibody against KIF4A (Bethyl Laboratories, Montgomery, TX), the mouse monoclonal antibody against MRE11A (GeneTex, San Antonio, TX) and the anti-lamin A/C rabbit polyclonal antibody (Cell Signaling Technology, Boston, MA). The anti-Huwei1 rabbit polyclonal antibody was a kind gift from Dr. S.S. Wing (McGill University, Montreal, Canada).

3T3-L1 adipogenesis assay. Differentiated mouse 3T3-L1 cells were fixed in formaldehyde for one hour and stained with 0.2% Oil Red O in 60% isopropanol for 30 min. Fixed cells were washed with water and incubated with fresh isopropanol. Released Oil red O was measured at 510 nm on a spectrophotometer. The Stealth small interference RNA specific for mouse *Wrn* mRNA (MSS212619: 5'-CCU CUG UUG GGA GUC AUC AAA CAU U-3') were purchased from Invitrogen Inc., (Burlington,

ON). 3T3-L1 cells were transfected with this siRNA using the Lipofectamine 2000 reagent (Invitrogen Inc., Burlington, ON).

Acknowledgements

We are grateful to Dr. D. Batchvarov (FRSQ-Réseau Cancer Core Genomic Facility, Quebec City, Canada) for the microarray hybridization and scanning experiments. We are also grateful to Dr. S.S. Wing (McGill University, Montreal, Canada) for the anti-Huwei1 antibody. J.V. holds a FQRNT post-doctoral fellowship. This work was supported by grants from the National Cancer Institute of Canada to J.-Y.M. and by the Natural Sciences and Engineering Research Council of Canada and the Canadian Institutes of Health Research to M.L.

Note

Supplementary materials can be found at:

www.landesbioscience.com/supplement/TuragaCC8-13-Sup.pdf

www.landesbioscience.com/supplement/TuragaCC8-13-Sup.xls

References

- Epstein CJ, Martin GM, Schultz AL, Motulsky AG. Werner's syndrome: a review of its symptomatology, natural history, pathologic features, genetics and relationship to the natural aging process. *Medicine* 1966; 45:177-221.
- Lebel M. Molecular mechanisms of Werner's syndrome. In: Lebel M, ed. *Textbook Cases*. Austin: RG Landes Co 2004; 1-156.
- Cheng WH, Muftuoglu M, Bohr VA. Werner syndrome protein: functions in the response to DNA damage and replication stress in S-phase. *Exp Gerontol* 2007; 42:871-8.
- Lee JY, Kozak M, Martin JD, Pennock E, Johnson FB. Evidence that a RecQ helicase slows senescence by resolving recombining telomeres. *PLoS Biol* 2007; 5:160.
- Balajee AS, Machwe A, May A, Gray MD, Oshima J, Martin GM, et al. The Werner syndrome protein is involved in RNA polymerase II transcription. *Mol Biol Cell* 1999; 10:2655-68.
- Blander G, Kipnis J, Leal JF, Yu CE, Schellenberg GD, Oren M. Physical and functional interaction between p53 and the Werner's syndrome protein. *J Biol Chem* 1999; 274:29463-9.
- Kyng KJ, May A, Kolvraa S, Bohr VA. Gene expression profiling in Werner syndrome closely resembles that of normal aging. *Proc Natl Acad Sci USA* 2003; 100:12259-64.
- Mukherjee AB, Costello C. Aneuploidy analysis in fibroblasts of human premature aging syndromes by FISH during in vitro cellular aging. *Mech Ageing Dev* 1998; 103:209-22.
- Melcher R, von Golitschek R, Steinlein C, Schindler D, Neitzel H, Kainer K, et al. Spectral karyotyping of Werner syndrome fibroblast cultures. *Cytogenet Cell Genet* 2000; 91:180-5.
- Turaga RVN, Massip L, Chavez A, Johnson FB, Lebel M. Werner syndrome protein prevents DNA breaks upon chromatin structure alteration. *Aging Cell* 2007; 6:471-81.
- Itahana K, Campisi J, Dimri GP. Methods to detect biomarkers of cellular senescence: the senescence-associated beta-galactosidase assay. *Methods Mol Biol* 2007; 371:21-31.
- Yamaguchi-Iwai Y, Sonoda E, Sasaki MS, Morrison C, Haraguchi T, Hiraoka Y, et al. Mre11 is essential for the maintenance of chromosomal DNA in vertebrate cells. *EMBO J* 1999; 18:6619-29.
- Subramanian A, Tamayo P, Mootha V, Mukherjee S, Ebert BL, Gillette MA, et al. Gene set enrichment analysis: a knowledge-based approach for interpreting genome-wide expression profiles. *Proc Natl Acad Sci USA* 2005; 102:15545-50.
- Wu Q, Kirschmeier P, Hockenberry T, Yang T, Brassard DL, Wang L, et al. Transcriptional regulation during p21^{WAF1/CIP1}-induced apoptosis in human ovarian cancer cells. *J Biol Chem* 2002; 277:36329-37.
- Goldrath AW, Luckey CJ, Park R, Benoist C, Mathis D. The molecular program induced in T cells undergoing homeostatic proliferation. *Proc Natl Acad Sci USA* 2004; 101:16885-90.
- Chang HY, Seddon JB, Alizadeh AA, Sood R, West RB, Montgomery K, et al. Gene expression signature of fibroblast serum response predicts human cancer progression: similarities between tumors and wounds. *PLoS Biol* 2004; 2:7.
- Lee MS, Hanspers K, Barker CS, Korn AP, McCune JM. Gene expression profiles during human CD4⁺ T cell differentiation. *Int Immunol* 2004; 16:1109-24.
- Jackson-Grusby L, Beard C, Possemato R, Tudor M, Fambrough D, Csankovszki G, et al. Loss of genomic methylation causes p53-dependent apoptosis and epigenetic deregulation. *Nat Genet* 2001; 27:31-9.
- Song YJ, Stinski MF. Effect of the human cytomegalovirus IE86 protein on expression of E2F-responsive genes: a DNA microarray analysis. *Proc Natl Acad Sci USA* 2002; 99:2836-41.
- Shepard JL, Amatruda JF, Stern HM, Subramanian A, Finkelstein D, Ziai J, et al. A zebrafish bmyb mutation causes genome instability and increased cancer susceptibility. *Proc Natl Acad Sci USA* 2005; 102:13194-9.
- Mariadason JM, Corner GA, Augenlicht LH. Genetic reprogramming in pathways of colonic cell maturation induced by short chain fatty acids: comparison with trichostatin A, sulindac and curcumin and implications for chemoprevention of colon cancer. *Cancer Res* 2000; 60:4561-72.
- Underhill GH, George D, Bremer EG, Kansas GS. Gene expression profiling reveals a highly specialized genetic program of plasma cells. *Blood* 2003; 101:4013-21.
- Hoffmann R, Seidl T, Neeb M, Rolink A, Melchers F. Changes in gene expression profiles in developing B cells of murine bone marrow. *Genome Res* 2002; 12:98-111.
- Ren B, Cam H, Takahashi Y, Volkert T, Terragni J, Young RA, et al. E2F integrates cell cycle progression with DNA repair, replication and G(2)/M checkpoints. *Genes Dev* 2002; 16:245-56.
- Vernell R, Helin K, Muller H. Identification of target genes of the p16^{INK4a}-pRB-E2F pathway. *J Biol Chem* 2003; 278:46124-37.
- Yu D, Cozma D, Park A, Thomas-Tikhonenko A. Functional validation of genes implicated in lymphomagenesis: an in vivo selection assay using a Myc-induced B-cell tumor. *Ann NY Acad Sci* 2005; 1059:145-59.
- Iritani BM, Delrow J, Grandori C, Gomez I, Klacking M, Carlos LS, et al. Modulation of T-lymphocyte development, growth and cell size by the Myc antagonist and transcriptional repressor Mad1. *EMBO J* 2002; 21:4820-30.
- Menssen A, Hermeking H. Characterization of the c-MYC-regulated transcriptome by SAGE: identification and analysis of c-MYC target genes. *Proc Natl Acad Sci USA* 2002; 99:6274-9.
- Greenbaum S, Lazorchak AS, Zhuang Y. Differential functions for the transcription factor E2A in positive and negative gene regulation in pre-B lymphocytes. *J Biol Chem* 2004; 279:45028-35.
- Kang HC, Kim IJ, Park JH, Shin Y, Ku JL, Jung MS, et al. Identification of genes with differential expression in acquired drug-resistant gastric cancer cells using high-density oligonucleotide microarrays. *Clin Cancer Res* 2004; 10:272-84.
- Hu T, Gibson DP, Carr GJ, Torontali SM, Tiesman JP, Chaney JG, et al. Identification of a gene expression profile that discriminates indirect-acting genotoxins from direct-acting genotoxins. *Mutat Res* 2004; 549:5-27.
- Gajate C, An F, Mollinedo F. Differential cytostatic and apoptotic effects of ecteinascidin-743 in cancer cells. Transcription-dependent cell cycle arrest and transcription-independent JNK and mitochondrial mediated apoptosis. *J Biol Chem* 2002; 277:41580-9.
- Marchini S, Marrazzo E, Bonomi R, Chiorino G, Zaffaroni M, Weissbach L, et al. Molecular characterization of two human cancer cell lines selected in vitro for their chemotherapeutic drug resistance to ET-743. *Eur J Cancer* 2005; 41:323-33.
- Brentani H, Caballero OL, Camargo AA, da Silva AM, da Silva WA Jr, Dias Neto E, et al. The generation and utilization of a cancer-oriented representation of the human transcriptome by using expressed sequence tags. *Proc Natl Acad Sci USA* 2003; 100:13418-23.
- Martinez N, Sanchez-Beato M, Carnero A, Moneo V, Tercero JC, Fernandez I, et al. Transcriptional signature of Ecteinascidin 743 (Yondelis, Trabectedin) in human sarcoma cells explanted from chemo-naïve patients. *Mol Cancer Ther* 2005; 4:814-23.
- Zhan F, Huang Y, Colla S, Stewart JP, Hanamura I, Gupta S, et al. The molecular classification of multiple myeloma. *Blood* 2006; 108:2020-8.
- Rhodes DR, Yu J, Shanker K, Deshpande N, Varambally R, Ghosh D, et al. Large-scale meta-analysis of cancer microarray data identifies common transcriptional profiles of neoplastic transformation and progression. *Proc Natl Acad Sci USA* 2004; 101:9309-14.
- Hedenfalk I, Ringner M, Ben-Dor A, Yakhini Z, Chen Y, Chebil B, et al. Molecular classification of familial non-BRCA1/BRCA2 breast cancer. *Proc Natl Acad Sci USA* 2003; 100:2532-7.
- Zhan F, Hardin J, Kordsmeier B, Bumm K, Zheng M, Tian E, et al. Global gene expression profiling of multiple myeloma, monoclonal gammopathy of undetermined significance, and normal bone marrow plasma cells. *Blood* 2002; 99:1745-57.
- Ferrando AA, Armstrong SA, Neuberger DS, Sallan SE, Silverman LB, Korsmeyer SJ, et al. Gene expression signatures in MLL-rearranged T-lineage and B-precursor acute leukemias: dominance of HOX dysregulation. *Blood* 2003; 102:262-8.
- Burton GR, Guan Y, Nagarajan R, McGehee RE Jr. Microarray analysis of gene expression during early adipocyte differentiation. *Gene* 2002; 293:21-31.
- Burton GR, Nagarajan R, Peterson CA, McGehee RE Jr. Microarray analysis of differentiation-specific gene expression during 3T3-L1 adipogenesis. *Gene* 2004; 329:167-85.
- Li Y, Lazar MA. Differential gene regulation by PPARgamma agonist and constitutively active PPARgamma2. *Mol Endocrinol* 2002; 16:1040-8.
- Chen C, Ouyang W, Grigora V, Zhou Q, Carnes K, Lim H, et al. ERM is required for transcriptional control of the spermatogonial stem cell niche. *Nature* 2005; 436:1030-4.
- Le N, Nagarajan R, Wang JY, Araki T, Schmidt RE, Milbrandt J. Analysis of congenital hypomyelinating Egr2Lo/Lo nerves identifies Sox2 as an inhibitor of Schwann cell differentiation and myelination. *Proc Natl Acad Sci USA* 2005; 102:2596-601.
- Mody M, Cao Y, Cui Z, Tay KY, Shyong A, Shimizu E, et al. Genome-wide gene expression profiles of the developing mouse hippocampus. *Proc Natl Acad Sci USA* 2001; 98:8862-7.
- Ly DH, Lockhart DJ, Lerner RA, Schultz PG. Mitotic misregulation and human aging. *Science* 2000; 287:2486-92.

48. Croonquist P, Linden M, Zhao F, Van Ness BG. Gene profiling of a myeloma cell line reveals similarities and unique signatures among IL-6 response, N-ras activating mutations, and coculture with bone marrow stromal cells. *Blood* 2003; 102:2581-92.
49. Tian B, Nowak DE, Jamaluddin M, Wang S, Brasier AR. Identification of direct genomic targets downstream of the nuclear factor-kappaB transcription factor mediating tumor necrosis factor signaling. *J Biol Chem* 2005; 280:17435-48.
50. Martinelli S, Urošević M, Daryadel A, Oberholzer PA, Baumann C, Fey MF, et al. Induction of genes mediating interferon-dependent extracellular trap formation during neutrophil differentiation. *J Biol Chem* 2004; 279:44123-32.
51. Browne EP, Wing B, Coleman D, Shenk T. Altered cellular mRNA levels in human cytomegalovirus-infected fibroblasts: viral block to the accumulation of antiviral mRNAs. *J Virol* 2001; 75:12319-30.
52. Xie X, Lu J, Kulbokas EJ, Golub TR, Mootha V, Lindblad-Toh K, et al. Systematic discovery of regulatory motifs in human promoters and 3' UTRs by comparison of several mammals. *Nature* 2005; 434:338-45.
53. Deschênes F, Massip L, Garand C, Lebel M. In vivo misregulation of genes involved in apoptosis, development and oxidative stress in mice lacking both functional Werner syndrome protein and poly(ADP-ribose) polymerase-1. *Hum Mol Genet* 2005; 14:3293-308.
54. Kudlow BA, Kennedy BK, Monnat RJ Jr. Werner and Hutchinson-Gilford progeria syndromes: mechanistic basis of human progeroid diseases. *Nat Rev Mol Cell Biol* 2007; 8:394-404.
55. Adelfalk C, Scherthan H, Hirsch-Kauffmann M, Schweiger M. Nuclear deformation characterizes Werner syndrome cells. *Cell Biol Int* 2005; 29:1032-7.
56. Spillare EA, Robles AI, Wang XW, Shen JC, Yu CE, Schellenberg GD, et al. p53-mediated apoptosis is attenuated in Werner syndrome cells. *Genes Dev* 1999; 13:1355-60.
57. Lombard DB, Beard C, Johnson FB, Marciniak RA, Dausman J, Bronson R, et al. Mutations in the WRN gene in mice accelerate mortality in a p53-null background. *Mol Cell Biol* 2000; 20:3286-91.
58. Grandori C, Wu KJ, Fernandez P, Ngouenet C, Grim J, Clurman BE, et al. Werner syndrome protein limits MYC-induced cellular senescence. *Genes Dev* 2003; 17:1569-74.
59. Adhikary S, Marinoni F, Hock A, Hulleman E, Popov N, Beier R, et al. The ubiquitin ligase HectH9 regulates transcriptional activation by Myc and is essential for tumor cell proliferation. *Cell* 2005; 123:409-21.
60. Opresko PL, Calvo JP, von Kobbe C. Role for the Werner syndrome protein in the promotion of tumor cell growth. *Mech Ageing Dev* 2007; 128:423-36.
61. Kyng KJ, Bohr VA. Gene expression and DNA repair in progeroid syndromes and human aging. *Ageing Res Rev* 2005; 4:579-602.
62. Cheng WH, Kusumoto R, Opresko PL, Sui X, Huang S, Nicolette ML, et al. Collaboration of Werner syndrome protein and BRCA1 in cellular responses to DNA interstrand cross-links. *Nucleic Acids Res* 2006; 34:2751-60.
63. De Stefano N, Dotti MT, Battisti C, Sicurelli F, Stromillo ML, Mortilla M, et al. MR evidence of structural and metabolic changes in brains of patients with Werner's syndrome. *J Neurol* 2003; 250:1169-73.
64. Leverenz JB, Yu CE, Schellenberg GD. Aging-associated neuropathology in Werner syndrome. *Acta Neuropathol (Berl)* 1998; 96:421-4.
65. Kakigi R, Endo C, Neshige R, Kohno H, Kuroda Y. Accelerated aging of the brain in Werner's syndrome. *Neurology* 1992; 42:922-4.
66. Mori S, Murano S, Yokote K, Takemoto M, Asaumi S, Take A, et al. Enhanced intra-abdominal visceral fat accumulation in patients with Werner's syndrome. *Int J Obes Relat Metab Disord* 2001; 25:292-5.
67. Davis T, Kipling D. Werner Syndrome as an example of inflamm-aging: possible therapeutic opportunities for a progeroid syndrome? *Rejuvenation Res* 2006; 9:402-7.
68. Adler AS, Sinha S, Kawahara TL, Zhang JY, Segal E, Chang HY. Motif module map reveals enforcement of aging by continual NFkappaB activity. *Genes Dev* 2007; 21:3244-57.
69. Laine JP, Opresko PL, Indig FE, Harrigan JA, von Kobbe C, Bohr VA. Werner protein stimulates topoisomerase I DNA relaxation activity. *Cancer Res* 2003; 63:7136-46.
70. Dimri GP, Lee X, Basile G, Acosta M, Scott G, Roskelley C, et al. A biomarker that identifies senescent human cells in culture and in aging skin in vivo. *Proc Natl Acad Sci USA* 1995; 92:9363-7.
71. Sambrook J, Fritsch EF, Maniatis T. *Molecular Cloning: A Laboratory Manual*. Cold Spring Harbor Laboratory Press, Plainview NY 1989.
72. Benjamini Y, Hochberg Y. Controlling the false discovery rate: a practical and powerful approach to multiple testing. *J R Stat Soc Series B* 1989; 57:289-300.